



## Computational Design and Analysis of a Novel Battery Thermal Management System of a Single 26650 Li-Ion Battery Cell for Electric Vehicle Application

Divya D Shetty<sup>1</sup>, Mahamad Sulthan<sup>1</sup>, Mohammad Zuber<sup>1</sup>, Irfan Anjum Badruddin<sup>2</sup>, Chandrakant R Kini<sup>1,\*</sup>

<sup>1</sup> Department of Aeronautical and Automobile Engineering, Manipal Institute of Technology, Manipal Academy of Higher Education, Manipal, Karnataka State, India

<sup>2</sup> Department of Mechanical Engineering, College of Engineering, King Khalid University, Saudi Arabia

### ARTICLE INFO

### ABSTRACT

#### Article history:

Received 18 November 2021

Received in revised form 30 January 2022

Accepted 5 February 2022

Available online 20 March 2022

#### Keywords:

Lithium-ion; Electric Vehicle; Battery Thermal Management System; Single cell

The adverse climate change has posed an emergency for the world to shift to green energy systems. The largest contributor for air pollution, which is the primary cause for the adverse climate change is the fossil fuel driven conventional vehicles. Therefore, electric vehicles are going to be the future of the automotive industry. Due to the abundance of lithium mineral and high-power density characteristics, lithium-ion powered electric vehicles are prominent choice. Similar to the vehicles driven by internal combustion engines, the electric vehicles should be able to travel long distances while carrying significantly heavy loads. This requires the battery to operate continuously for long duration under heavy loads, which results in increase of battery temperatures beyond the normal operating range. High battery temperature will degrade its performance and subsequently deteriorate battery life. Therefore, it is important to ensure that the battery temperature lies well within normal range for all possible operating conditions of the electric vehicle. This can be achieved by adopting a suitable Battery Thermal Management System (BTMS). In the present study, computational analysis of a single Lithium-ion (LiCoO<sub>2</sub> 26650) cell designed based on Newman, Tiedemann, Gu and Kim (NTGK) formulation has been carried out to evaluate the maximum temperature attained by the cell. Furthermore, a BTMS is designed for the same using a novel liquid cooling plate (containing three channels) which is in contact with the cell surface. The maximum temperature attained by the cell with BTMS at different discharge rates of 0.5 C, 1.0 C and 1.5 C is determined. To enhance cooling, two fins are attached on top of the liquid cooling plate. Water is used as coolant and analysis is carried out for 0.01 m<sup>3</sup>/s flow rate. The maximum temperatures attained by the cell with and without BTMS are found to be 313.72 K, 307.37 K, 302.31 K and 298.55 K, 298.52 K, 297.41 K at discharge rates of 1.5 C, 1.0 C and 0.5 C. Therefore, with BTMS the maximum cell temperature attained is 39%, 25% and 16% less compared to the bare cell, which indicates that the BTMS adopted in the present work is significantly effective in controlling rise in maximum cell temperature.

\* Corresponding author.

E-mail address: [chandra.kini@manipal.edu](mailto:chandra.kini@manipal.edu)

<https://doi.org/10.37934/arfmts.93.2.6175>

## 1. Introduction

In the present world scenario, adverse climate change has become a major concern, which is primarily caused due to air pollution. Large emissions of greenhouse gases resulted in global warming and rise in average temperature of the earth. The major contributor for greenhouse gases is the transport sector, which accounts for about 21% of total emission out of which 15% is from road transport sector i.e., from the conventional vehicles driven by internal combustion engines [1]. Hence, to combat air pollution use of electric vehicles and hybrid electric vehicle systems has become a prominent option. However, primary challenge with electric vehicles is to enhance the performance of its energy storage system that is commonly a lithium-ion (Li-ion) battery [2]. The performance of Li-ion battery is predominantly dependent on its operating temperature. For optimum performance, it is recommended to maintain its operating temperature in the range of 15 to 35 °C. In addition, the temperature difference between individual cells in a battery pack should be less than 5 °C. This will help to maintain optimum balance between the battery life and battery performance [3]. To evade early degradation of battery capacity and thermal runaway, its temperature should be maintained within 60 °C to 80 °C. In-depth research on Li-ion batteries are required and several critical parameters such as battery cycle life and full discharge cycle needs to be thoroughly understood which in turn will help in designing an efficient Battery Thermal Management System (BTMS) for further enhancing its performance characteristics [4].

To design an effective BTMS for Li-ion battery, it is important to understand temperature distribution of the cell. Several numerical studies have been accomplished on different cell models such as thermal model, electrochemical model, Equivalent Circuit Model (ECM) [5]. The main inputs for Li-ion battery thermal model are thermal properties and battery heat generation rate. This model can be either 1-D, 2-D or 3-D system. In the lumped thermal model, the temperature gradient inside the battery cell is considered to be negligible and thus it simulates the entire cell at uniform temperature. Furthermore, it helps to evaluate the surface and core temperature of the cell incorporating the internal thermal resistance and battery pack degradation [6]. Bryden *et al.*, [7] have evaluated the heat capacity of different types of Li-ion cell and determined the total resistance in the circuit. Coman *et al.*, [8] have studied the thermal runaway of lithium cobalt oxide battery and Lin *et al.*, [9] has developed an electro-chemical model for a Li-ion battery. These studies are predominantly based on lumped models of small sized Li-ion batteries. However, for large batteries it is even important to explore the cooling parameters. In big sized Li-ion batteries, the temperature gradient across the cell is substantially large and the maximum temperature attained is also significant. Hence, BTMS is extremely essential for large Li-ion batteries. Panchal *et al.*, [10] perceived that when a 20 Ah Li-ion battery is discharged at different discharge rate of 2 C, 3 C and 4 C, there exists a non-uniform temperature distribution across the cell. Samba *et al.*, [11] has developed a 2-D model of a pouch battery to study the temperature distribution. Further, an analytical method is developed to evaluate the heat conduction inside the Li-ion battery.

Three dimensional computational models have been used by several researchers to investigate the thermal performance of a single cell and later the same is applied to develop battery pack [12]. Electrochemical battery models are resolved using Multi-Scale Multi-Domain (MSMD) approach which basically rely upon electrochemical equation characterizing the flow of ions in different domains and scales. This approach will determine the cell temperature distribution, heat generation, voltage and current characteristics of the cell. ANSYS Fluent is used to perform the analysis with three different sub-models viz. Equivalent Circuit Model (ECM), Newman Pseudo-2D Model and Newman, Tiedemann, Gu and Kim (NTGK) model [13]. ECM is mainly used to study battery's electric behaviour which has inbuilt electric circuit [14]. Newman Pseudo-2D model is based on the physics of electrodes

and electrolyte, which can capture Li-ion movement in circuit. NTGK model is a semi-empirical electrochemical model which can simulate temperature rise in the cell. Using this model, the difference in computational and experimental values of cell temperature is found to be less than 1°C [13]. Besides, MSMD model can be used to simulate large battery pack with the cell connected in series as well as parallel. With MSMD model, it is possible to simulate thermal runaway of any cell and related consequences. Panchal *et al.*, [15] have investigated the voltage and temperature rise of a 26650-lithium phosphate battery using MSMD model at constant discharge rates. G. Li *et al.*, [14] has simulated the performance of prismatic battery using similar approach. Zhou *et al.*, [16] have studied thermal control of cylindrical Li-ion batteries. To ensure optimal performance and safety of Li-ion batteries it is important to design an appropriate Battery Thermal Management System.

Different types of thermal management system such as air cooled, liquid cooled, heat pipe containing phase change materials and hybrid cooling systems are employed for Li-ion batteries used in electric vehicles [2]. The major disadvantage of air based BTMS is that it consumes more power due to low thermal conductivity of air. Moreover, the temperature distribution is non-uniform throughout the battery pack which further deteriorates the battery performance [17]. Compared to air cooled BTMS, liquid-based cooling technology provides better cooling ability. Commonly used liquid cooling systems adopts cooling channels between the cells and in some cases the battery cell is directly immersed in the cooling medium. Several designs of liquid cooling systems such as cooling plates with mini-channel structures, serpentine cooling channels are found to be highly efficient and compact in structure [18]. The commonly used heat transfer fluids in BTMS are water, ethylene glycol, mineral oil, refrigerants and dielectric fluids [19]. The operating parameters of the cold plate generally depends on type, shape and size of cooling channel as well as coolant flow path. Meanwhile, the cooling systems based on phase change material depends upon the physical property of the material can be used for BTM in electric vehicles [20].

The drawback of using PCM based cooling system is that they possess low thermal conductivity and hence it responds slowly at high thermal loads. The other disadvantages of PCM are poor mechanical characteristics, leakage and low heat transfer rate between PCM and surrounding. Researchers are working on enhancing the thermal conductivity of PCM by introducing metal particles or metal foams but still additional cooling is required along with PCM for optimum performance of the battery [21]. Heat pipes can efficiently remove heat from battery, however, it is similar to PCM technology and does require additional cooling system alongside. Further research is required to use heat pipes as a potential technology for BTMS application [22]. In designing a liquid cooled thermal management system, various factors such as weight of system, space, operating cost, possibility of leakage, possible resistance between the cold plate and Li-ion cell have to be thoroughly considered [20]. An optimum cooling plate should be highly efficient, compact in size, low cost, highly uniform and light weight. It is recommended to deploy computation models to select optimized cooling plate [23].

Zhao *et al.*, [24] has designed a liquid mini-channel thermal management system for cylindrical batteries and investigated the effect of different parameters such as number of channels, mass flow rate, size of fluid inlet and flow direction on performance of thermal management system. It is found that at an optimized mass flow rate of 10-3 kg/s with four mini channels can regulate the temperature below 40°C. Panchal *et al.*, [25] has investigated the performance of mini-channel cold plate using water as cooling medium for prismatic batteries. The study was conducted for battery discharge rates of 1 C and 2 C and different coolant temperatures of 5°C, 15°C and 25°C. It is observed from the outcome that as the battery discharge rate increases the temperature inside the cooling channel also increases. Huo *et al.*, [26] has explored the influence of fluid flow path, number of mini-channels and ambient temperature on thermal management system using a 3-D model of liquid cooled mini-

channel plate for EV batteries. It is seen that with increase in number of cooling channels and coolant mass flow rate, the battery temperature decreases. It has been also observed that the coolant flow path has very little influence on cooling efficiency compared to coolant flow rate. Jin *et al.*, developed and innovative cooling plate consisting of active and passive cooling components to provide a uniform battery thermal management. The cooling plate was integrated with phase change material and a fluid passage. As a result, it is observed that hybrid cooling plate was able maintain battery temperature below 40°C at 0.5C and 1.5C discharge rate.

Akbarzadeh *et al.*, studied the performance of hybrid cooling plate with PCM, which is 36% lighter than traditional liquid cooling plate. The result shows that by in co-operating hybrid liquid cooling plate the power consumption by the pump used to circulate the coolant decreases by 30%. It also helps in maintaining temperature uniformity all over the battery pack. Prajapati *et al.*, [27] have analysed the efficiency of three different micro-channels viz. identical cross-section, diverging cross-section and microchannel containing oblique fin. The oblique finned structured exhibit high heat transfers co-efficient compared to the other two microchannel. From the overview of literature, it is evident that the structure of cooling channel is an important factor influencing the heat transfer characteristics. Since in majority cases the inlet, outlet, area as well as thickness of the cooling plate is restricted by the battery pack design, optimization of the BTMS is critical and highly essential.

Hence, in order to design an efficient liquid cooled BTMS, it is essential to design a computational model and analyze the performance of single cell and obtain information on heat generation and maximum temperature attained. The present study focuses on developing a thermal model of cylindrical Li-ion battery to estimate the thermal parameters viz. temperature distribution, maximum temperature at different discharge rate. Further, to enhance the cooling performance and attain uniformity in temperature distribution, fins are adopted for the aforementioned cooling plate. The proposed method will help to maintain the operating temperature of Li-ion battery for electric vehicle applications within the optimized range.

## 2. Methodology

A CFD model of 26650 Lithium Cobalt Oxide (LiCoO<sub>2</sub>) cell is developed in this study. The thermal behaviour of the Li-ion cell is numerically evaluated using dual potential Newman, Tiedemann, Gu and Kim (NTGK) formulation. The simulation is performed at different constant current discharge rates.

### 2.1 Battery Geometry and Meshing

The cell used in the present work is a solid cylinder of 26 mm diameter and 65 mm length. For NTGK formulation, the cell is divided into three main components i.e., anode as negative tab, cathode as positive tab and the middle component as jelly roll. In reality, the cell will be covered with outer shell material but for simplifying the model, the thermal resistance of the outer shell is neglected and hence the outer shell is not included in the model. The battery cell with cooling cell model is shown in Figure 1.

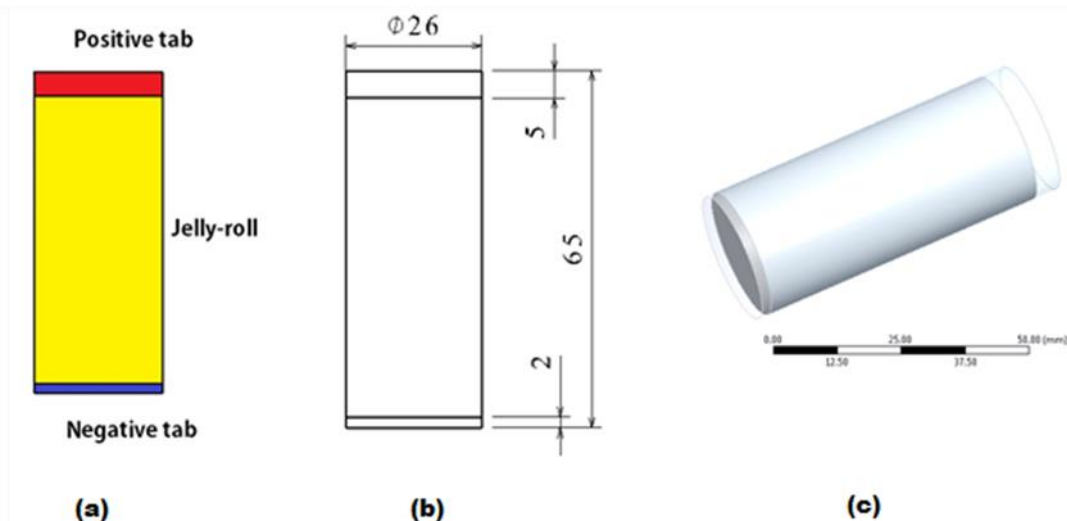


**Fig. 1.** NTGK Li-ion cell details (a) Cell components (b) Cell dimensions (c) Single cell battery model

Geometrical model of cooling system for single cell battery is developed using Ansys design modeller. The fins and cooling plate are modelled as solid domain and coolant channel as fluid domain. The fins are made of aluminium material and is connected to the top surface of cooling plate. The cooling plate has three internal coolant flow channels as shown in Figure 2. The dimension of cooling system is provided in Figure 2. Bottom surface of negative tab lies 3 mm above the cooling surface. The aluminium fins are in direct contact with the Li-ion cell. Heat is absorbed by the fins and transferred to the coolant passing through the channel beneath at a flow rate of  $0.01 \text{ m}^3/\text{s}$ .

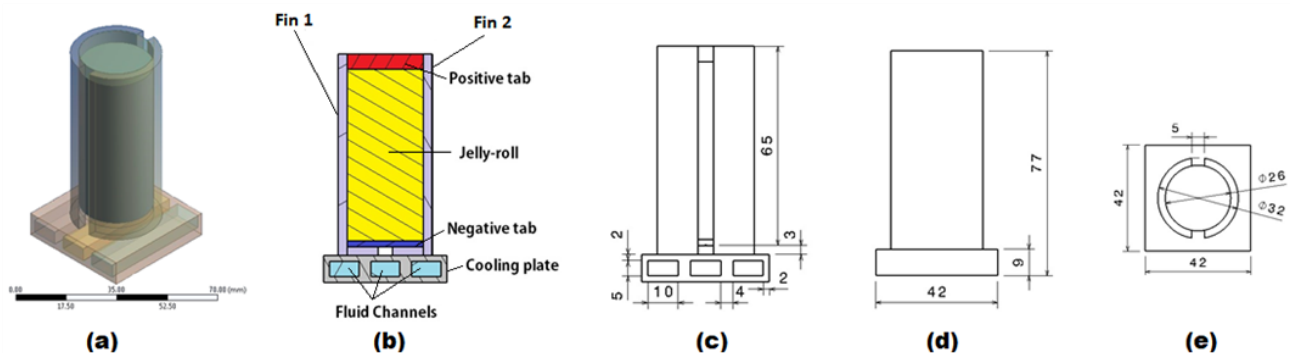


**Fig. 2.** Single cell with cooling system (a) Model of the cell with cooling system (b) Schematic of cooling system depicting various components (c) Front view (d) Side view (e) Top view

Mesh independence tests have been carried out to solve the NTGK single cell model with and without cooling at constant discharge current of 6 Amperes. For each case, the optimum mesh size is found to be 1.15 mm considering maximum temperature rise as the parameter of interest. Thus, mesh with 38988 elements is chosen for single cell without cooling and mesh with 258964 elements is selected for single cell with cooling NTGK model. The mesh metrics for both the cases are provided in Table 1 and 2.

**Table 1**  
Mesh metrics for single cell battery model

| Parameter          | Maximum | Minimum                 | Average                 |
|--------------------|---------|-------------------------|-------------------------|
| Element Quality    | 0.99752 | 0.63504                 | 0.90663                 |
| Aspect Ratio       | 2.8774  | 1.0511                  | 1.4965                  |
| Skewness           | 0.46674 | $3.8227 \times 10^{-3}$ | $9.2325 \times 10^{-2}$ |
| Orthogonal quality | 0.99998 | 0.81467                 | 0.98615                 |

**Table 2**  
Mesh metrics for cell with cooling system

| Parameter          | Maximum | Minimum                 | Average |
|--------------------|---------|-------------------------|---------|
| Element Quality    | 1       | $5.8996 \times 10^{-2}$ | 0.65168 |
| Aspect Ratio       | 31.191  | 1                       | 6.4128  |
| Skewness           | 0.50179 | $4.385 \times 10^{-6}$  | 0.14252 |
| Orthogonal quality | 1       | 0.70711                 | 0.94278 |

## 2.2. Equations Used in Numerical Analysis of The Battery Model

In the present work, Dual Potential Multi Scale-Multi Domain approach with NTGK electrochemical sub model is adopted for analysis of li-ion battery cell. The electrical and thermal field characteristics of the battery are solved in the computational domain at the battery's cell scale as follows [28]:

$$\frac{\partial(\rho C_p T)}{\partial t} - \nabla \cdot (k_c \Delta T) = \sigma_{pos} |\nabla \phi_{pos}|^2 + \sigma_{neg} |\nabla \phi_{neg}|^2 + \dot{q}_{E_{ch}} + \dot{q}_{short} \quad (1)$$

$$\left. \begin{aligned} \nabla \cdot (\sigma_{pos} \nabla \phi_{pos}) &= -(j_{E_{ch}} - j_{short}) \\ \nabla \cdot (\sigma_{neg} \nabla \phi_{neg}) &= (j_{E_{ch}} - j_{short}) \end{aligned} \right\} \quad (2)$$

where  $\phi$  is phase potential,  $\sigma$  is effective electric conductivity at electrodes,  $\dot{q}_{E_{ch}}$  and  $j_{E_{ch}}$  are the electrochemical reaction heat due to electrochemical reactions and volumetric current transfer rate respectively,  $\dot{q}_{short}$  and  $j_{short}$  are the heat generation rate due to battery internal short-circuit and current transfer rate respectively. The suffixes *pos*, *neg* represents positive and negative electrode. The source terms  $j_{E_{ch}}$  and  $\dot{q}_{E_{ch}}$  are calculated based on the electrochemical sub-model which is NTGK in the present case. NTGK is a simple semi-empirical electrochemical model.

The volumetric current transfer rate is related to potential field by:

$$j = \frac{C_N}{C_{ref} Vol} Y \left[ U - (\phi_{pos} - \phi_{neg}) \right] \quad (3)$$

where *Vol* is volume of active zone,  $C_{ref}$  is the battery capacity used to get *U* and *Y* parameter functions

Deep of discharge (DoD) is calculated as follows:

$$DoD = \frac{Vol}{3600Q_{nominal}} \int_0^t j dt \quad (4)$$

Depending on Deep of discharge, the  $U$  and  $Y$  parameter functions are evaluated as follows,

$$\left. \begin{aligned} U &= \left\{ \sum_{n=0}^5 a_n (DoD)^n \right\} - C_2 (T - T_{ref}) \\ Y &= \left\{ \sum_{n=0}^5 b_n (DoD)^n \right\} \exp \left( -C_1 \left\{ \frac{1}{T} - (1)T_{ref} \right\} \right) \end{aligned} \right\} \quad (5)$$

Where  $C_1$  and  $C_2$  are constants for a particular battery and  $T_{ref}$  is the reference temperature.

The Electro-Chemical reaction heat is given by,

$$q_{E_{ch}} = j_{E_{ch}} \left[ U - (\varphi_+ - \varphi_-) - T \frac{dU}{dT} \right] \quad (6)$$

where the first term in (6) represents heat due to over potential and second term represents entropy-based heat generation.

The Li-ion cell specifications, material properties for NTGK model, U and Y coefficients and cooling system material properties are listed in Table 3 to 6 respectively.

**Table 3**  
 LiCoO<sub>2</sub> 26650 Li-ion cell specifications

|                           |                    |
|---------------------------|--------------------|
| Anode material            | Graphite           |
| Cathode material          | LiCoO <sub>2</sub> |
| Mass                      | 0.088kg            |
| Height                    | 65mm               |
| Diameter                  | 26mm               |
| Emissivity                | 0.8                |
| Nominal voltage           | 3.70V              |
| Charging voltage limit    | 4.20V              |
| Cut-off voltage           | 2.75V              |
| Maximum discharge current | 2C                 |
| Maximum charge current    | 1C                 |
| Nominal capacity          | 4 Ah               |

**Table 4**  
 Material properties for NTGK model

| Properties                    | Jelly roll<br>(Active Zone)                 | Aluminium<br>(Positive Tab) | Steel<br>(Negative Tab) |
|-------------------------------|---|-----------------------------|-------------------------|
| Density (kg/m <sup>3</sup> )  | 2226  | 2719                        | 8030.0                  |
| Specific heat (J/kg-K)        | 1197  | 871                         | 502.480                 |
| Thermal conductivity (W/mK)   | 27  | 202.4                       | 16.27                   |
| Electrical conductivity (S/m) | 1.19×10 <sup>6</sup> , 9.83×10 <sup>5</sup> | 3.541×10 <sup>7</sup>       | 8.33×10 <sup>6</sup>    |

**Table 5**  
 U and Y coefficients for NTGK model

| Function | Coefficients |          |          |          |          |           |
|----------|--------------|----------|----------|----------|----------|-----------|
| $U$      | $a_0$        | $a_1$    | $a_2$    | $a_3$    | $a_4$    | $a_5$     |
|          | 4.0682       | -1.2669  | -0.9072  | 3.7550   | -2.3108  | -0.1701   |
| $Y$      | $b_0$        | $b_1$    | $b_2$    | $b_3$    | $b_4$    | $b_5$     |
|          | 16.5066      | -27.0367 | 237.3297 | -632.603 | 725.0825 | -309.8760 |

**Table 6**  
 Material property of cooling system

| Property                     | Fins (Aluminium) | Cooling plate (Aluminium) | Fluid Channel (Water) |
|------------------------------|------------------|---------------------------|-----------------------|
| Density (kg/m <sup>3</sup> ) | 2719.0           | 2719                      | 1000                  |
| Specific heat (J/kg-K)       | 871.0            | 871                       | 4184                  |
| Thermal conductivity (W/m-K) | 202.4            | 202.4                     | 0.6                   |

### 2.3 Boundary Conditions for Single Cell Battery

For the single cell battery, boundary conditions are applied to the cell wall, positive tab wall and negative tab wall, as given in the Table 7. Boundary conditions are varied for different discharge current rates.

**Table 7**  
 Single cell boundary conditions

| Current (A) | Heat Transfer Coefficient (W/m <sup>2</sup> k) | Free Stream Temperature (K) |
|-------------|--|-----------------------------|
| 2           | 3.6  | 297                         |
| 4           | 5.6  | 297                         |
| 6           | 7.7  | 296                         |

### 2.4 Boundary Conditions for BTMS

For BTMS, the value of inlet velocity and inlet temperature is varied. Finally, optimal values for inlet velocity and temperature is selected by conducting simulation for range given in Table 8. However, the cell boundary conditions remain the same as mentioned in Table 7.

**Table 8**  
 BTMS boundary conditions

| Current (A)                         | 2                       | 4   | 6   |
|-------------------------------------|-------------------------|-----|-----|
| Ambient temperature (K)             | 297                     | 297 | 296 |
| Fin Cooling plate temperature (K)   | 297                     | 297 | 296 |
| Fluid channel inlet temperature (K) | 297-300                 |     |     |
| Coolant/solid interface             | Conjugate heat transfer |     |     |
| Fluid channel inlet velocity(m/s)   | 0.005 – 0.1             |     |     |
| Cell initial temperature (K)        | 297                     | 297 | 296 |
| Fluid channel outlet pressure (Pa)  | 0 (gauge)               |     |     |



### 3. Result and Discussions

The cell behaviour when being discharged at different rates is computed by equation and NTGK model. The temperature rise in the cell is represented in Figure 3. The temperature tends to increase with the increase in discharge rate. The simulation results obtained for single cell without cooling is validated with the experimental results by [29] and found to be well within acceptable limits.

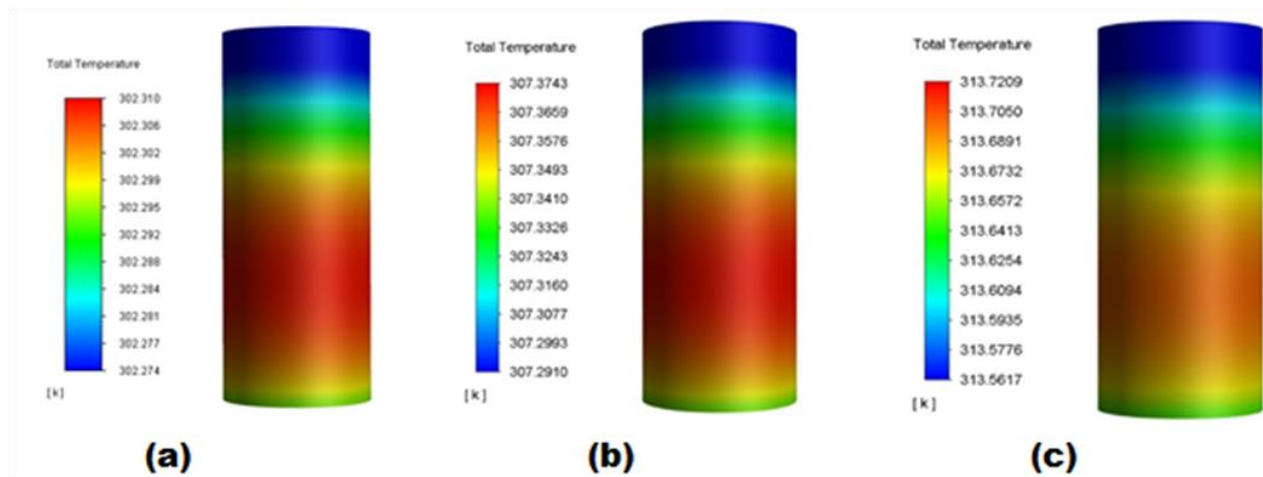


Fig. 3. Temperature contour of the cell at different discharge rates (a) 0.5 C (b) 1.0 C (c) 1.5 C

#### 3.1 Single Cell Without Cooling

Using the Ansys Workbench, the C-rate for three different discharge modules of 0.5 C, 1.0 C and 1.5 C has been analysed on the LiCoO<sub>2</sub> 26650 Li-ion battery. The maximum temperature of the cell was observed to be 313.95 K, 307.95 K, and 302.45 K for 1.5 C, 1.0 C and 0.5 C discharge rates respectively. Temperature rise in the cell for different discharge currents is shown in the Figure 4. The temperature of the cell increases as the internal heat generation increases due to the electrochemical reaction taking place inside the battery cell with time. The maximum temperature attained by the cell is found to be highest for 1.5 C discharge rate, which is because high current drawn at a relatively short time. With increase in discharge current rate, the battery temperature increases and the usage available time is significantly reduced as shown in Figure 4. A comparison of voltage drop at three different discharge modules is shown in Figure 5. It is clear from the graph that as discharge rate increases, temperature as well as voltage drop increase. It is observed that 313.95K is the maximum temperature attained by the cell at 1.5 C discharge rate due to high internal resistance and the charge is completely drained within 2500 seconds at same discharge rate.

Figure 4 and 5 shows the comparison between simulation results and experimental work. It can be observed that as the cell discharge rate increases the temperature rise also increases. At a discharge rate of 1.5 C the cell attains maximum temperature of 313.95 K which exceeds the optimum temperature. Hence, it is important to reduce this temperature by adopting BTMS. The deviation between experimental and simulation temperature values are found to be 0.2903 K, 0.6783 K and 0.3477 K for 0.5 C, 1.0 C and 1.5 C discharge rates respectively. This is due to the variation in ambient temperature during the experiment. These changes will continuously vary during the day which will lead to deviations in the experimental results whereas, the outcome of simulation usually remains steady. Therefore, these variations are neglected when comparing with computational results. This study will help to further compare the performance of single cell with cooling and without cooling.

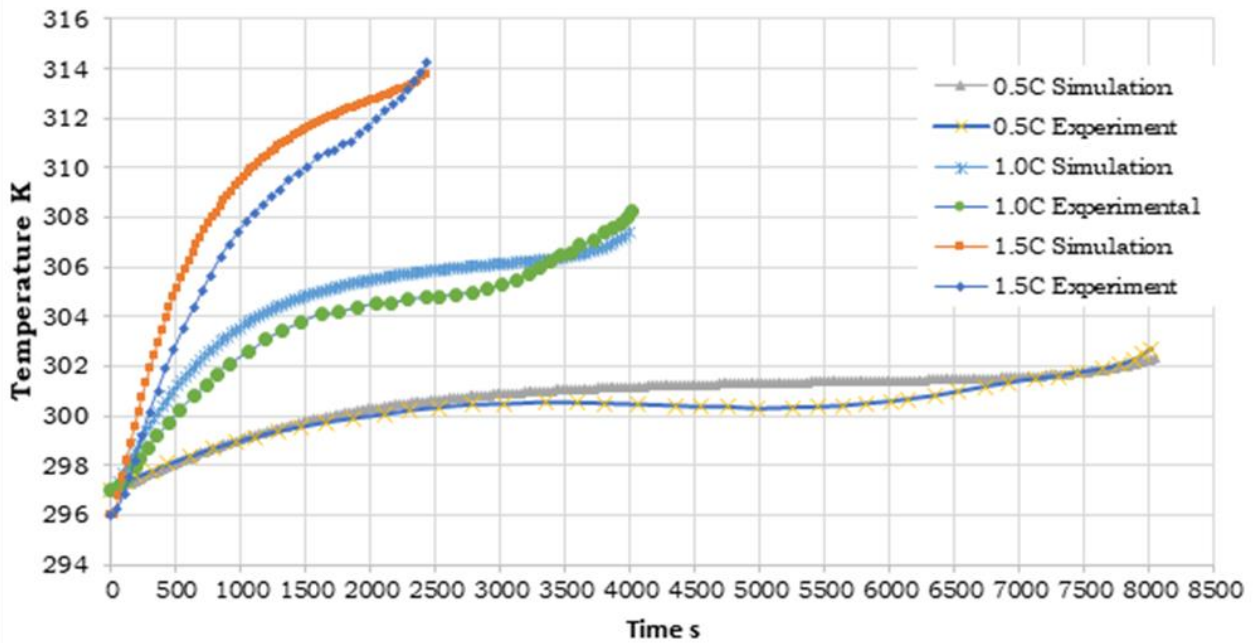


Fig. 4. Temperature variation at different discharge rates

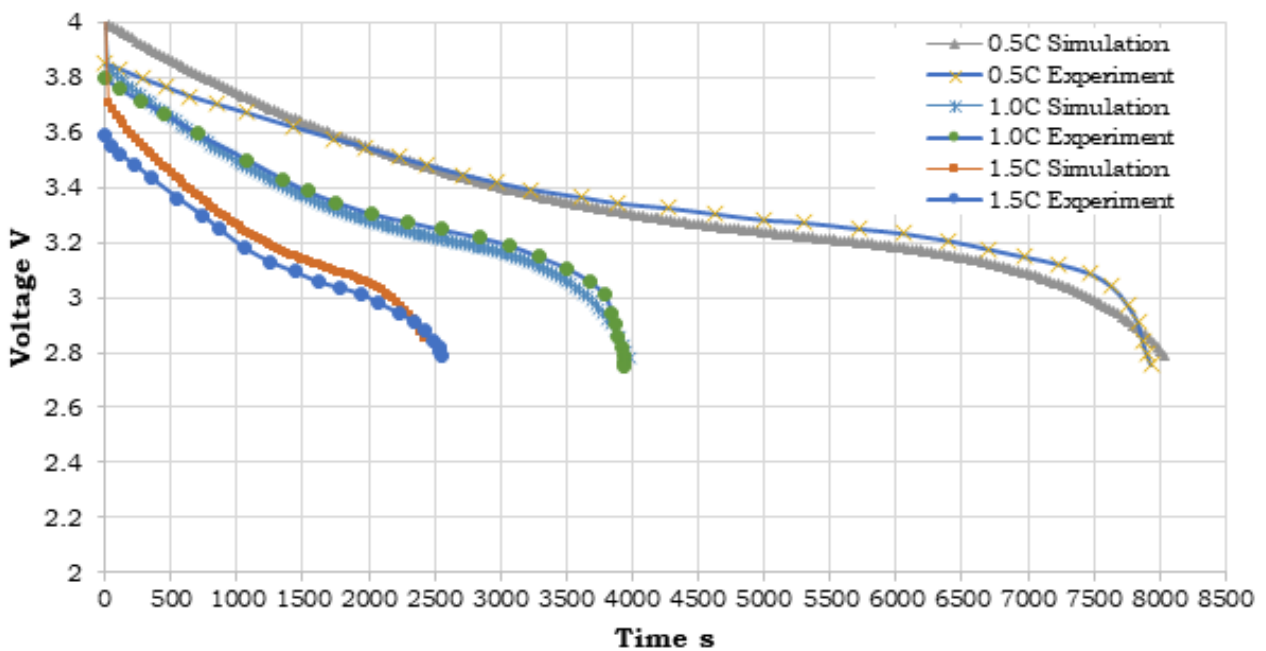
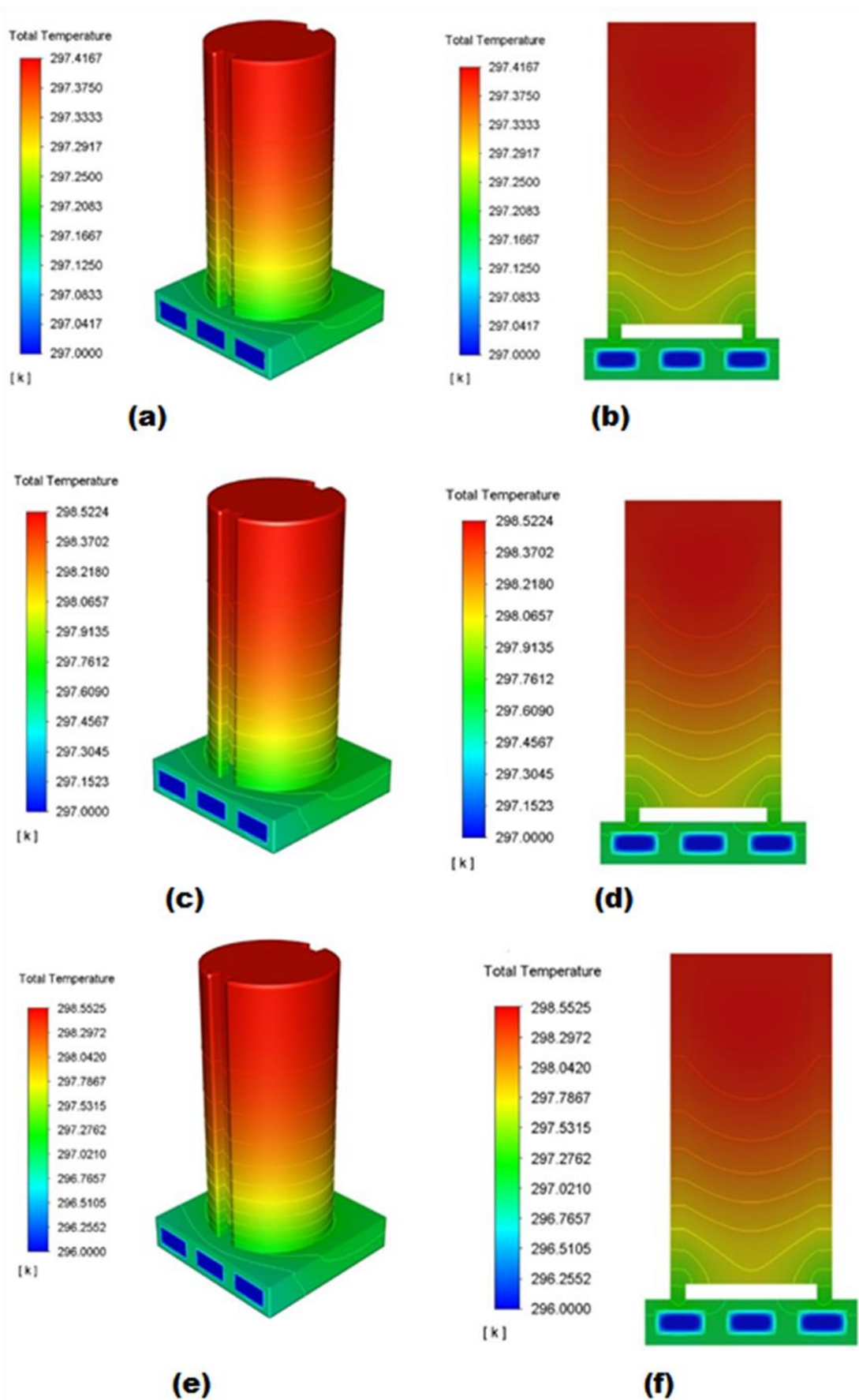


Fig. 5. Battery cell voltage variation at different discharge rates

### 3.2 Single Cell With BTMS

Figure 6 shows the temperature contour of single cell with cooling for three different discharge rates 0.5 C, 1.0 C and 1.5 C. The maximum temperature for discharge rates 0.5 C, 1.0 C and 1.5 C are 297.42 K, 298.52 K and 298.55 K respectively. From the temperature contours, it can be observed that bottom part of the cell is cooler compared to the top part because the cooling plate is attached to bottom of the fins. The temperature difference between top and bottom parts is considerably less.



**Fig. 6.** Temperature contour of cell with thermal management system at (a) 0.5 C (c) 1.0 C (e) 1.5 C and display of cut sections (b) 0.5 C (d) 1.0 C (f) 1.5 C

### 3.3 Comparison of Performance of Single Cell with Cooling (BTMS) and Without Cooling

Figure 7, 8 and 9 depicts the variation of cell temperature with time for discharge rates of 1.5 C, 1.0 C and 0.5 C respectively. From these graphs, it can be inferred that there is significant change in temperature when the thermal management system consisting of finned cooling plate is incorporated with single cell battery. All these factors contribute in decreasing the battery temperature and thus increases the battery lifespan. Such system also helps in preventing battery thermal runaway. In all these cases, battery starts at base temperature of around 296 to 298 K. The highest temperature the cell would attain without the cooling depends upon the discharge rates set for the battery. Higher the discharge rates, higher the cell temperature before total discharge.

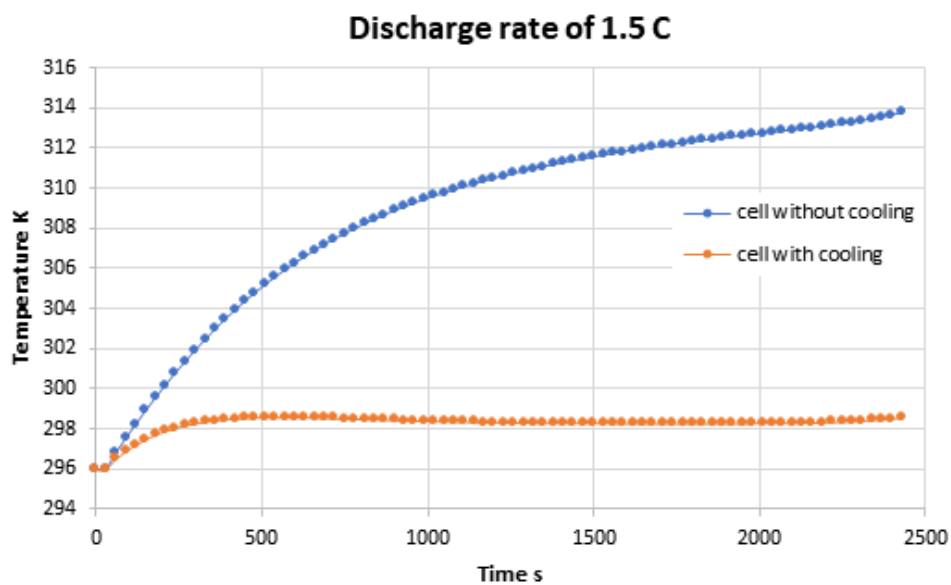


**Fig. 7.** Comparison of cell temperature with cooling and without cooling at 1.5 C discharge rate

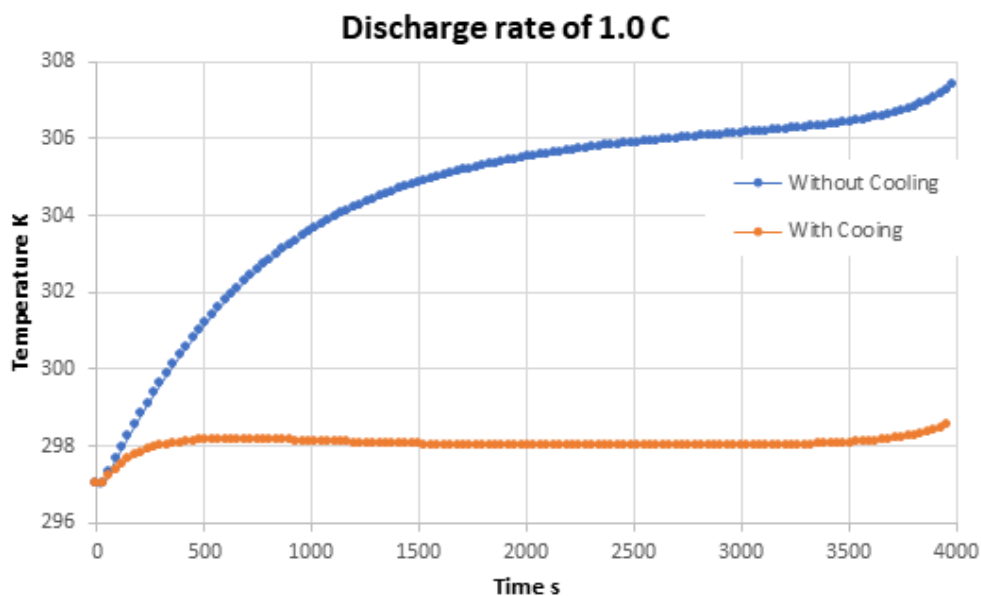


**Fig. 8.** Comparison of cell temperature with cooling and without cooling at 1.0 C discharge rate

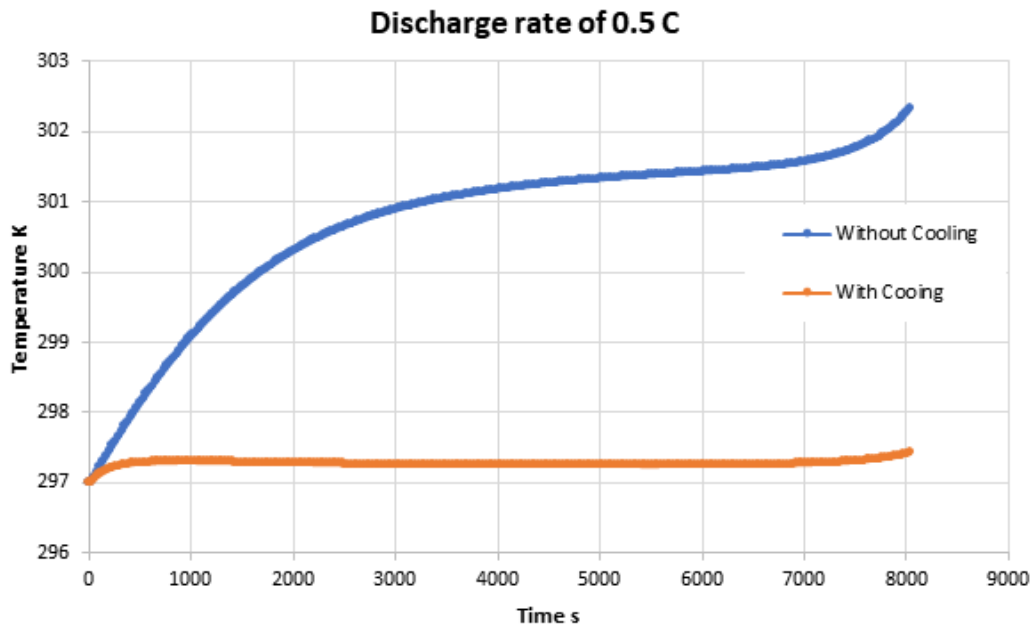


**Fig. 9.** Comparison of cell temperature with cooling and without cooling at 0.5 C discharge rate

For the discharge rate of 1.5 C, the maximum temperature of cell is 314 K without cooling, and with adoption of BTMS it would reach around 298 K. Similarly, for discharge rates of 1.0 C and 0.5 C the maximum temperature attained by cell without cooling are found to be 307.37 K and 302.31 K, and correspondingly 298.5 K and 297.42 K with cooling. Incorporating thermal management system will decrease the maximum temperature attained by 39%, 25% and 16% respectively at discharge rates of 1.5 C, 1.0 C and 0.5 C. The maximum temperature recorded in a single cell with cooling and without cooling is summarized in Table 9.

**Table 9**

Outcome of CFD analysis of single cell Li-ion battery with and without BTMS

| Discharge rate (C) | Initial cell temperature (K) | Maximum temperature rise without cooling (K) | Maximum temperature rise with cooling (K) |
|--------------------|------------------------------|--|---|
| 0.5                | 297                          | 302.31                                       | 297.42                                    |
| 1.0                | 297                          | 307.37                                       | 298.52                                    |
| 1.5                | 296                          | 313.73                                       | 298.56                                    |

### 3.4 Limitations of Present Work

The present work is modelling of single cell and designing the battery thermal management for the same. The battery thermal management proposed here is capable of maintaining single cell with in safe operating range of temperature. The arrays of cell can be modelled using the same method and apply the battery thermal management to it. The effect of different flowrates on the cooling performance of BTMS must be studied. Optimization of cooling channel is also necessary before applying it to arrays of cell.

## 4. Conclusions

In the present work CFD analysis has been carried out on a single 26650 LiCoCO<sub>2</sub> cell for electric vehicle application. The dual potential NTGK model is used for simulation. The simulation results are

validated against experimental work available in literature and is found to be well within acceptable limits. The variation of cell temperature and voltage with time for single cell without cooling has been evaluated at different discharge rates of 2A (0.5 C), 4A (1.0 C) and 6A (1.5 C). Furthermore, a finned cooling plate with water as coolant has been used to regulate the maximum temperature attained by the cell. Maximum temperature attained by the cell with and without cooling has been simulated at various constant current discharge rates. The outcome of the simulation study is summarized below

- i. Single cell without cooling attains maximum temperature of 313.72 K, 307.37 K and 302.31 K at discharge rates of 1.5 C, 1.0 C and 0.5 C respectively.
- ii. Single cell with Battery Thermal Management System (BTMS) it is observed that the maximum temperature attained by the cell is 298.55 K, 298.52 K and 297.41 K at discharge rate of 1.5 C, 1.0 C and 0.5 C respectively.
- iii. Compared to bare cell, the cell with BTMS reduces the maximum temperature reached by 39%, 25% and 16% at discharge rates of 1.5 C, 1.0 C and 0.5 C respectively thus implying that the BTMS adopted in the present study is effective.

### Acknowledgments

The authors thank the Department of Aeronautical and Automobile Engineering, Manipal Institute of Technology, Manipal Academy, Manipal for providing the computational facility to carry out this research.

### References

- [1] Martins, Florinda, Carlos Felgueiras, Miroslava Smitkova, and Nídia Caetano. "Analysis of fossil fuel energy consumption and environmental impacts in European countries." *Energies* 12, no. 6 (2019): 964. <https://doi.org/10.3390/en12060964>
- [2] Perera, Frederica. "Pollution from fossil-fuel combustion is the leading environmental threat to global pediatric health and equity: Solutions exist." *International journal of environmental research and public health* 15, no. 1 (2018): 16. <https://doi.org/10.3390/ijerph15010016>
- [3] Cicconi, Paolo, Michele Germani, and Daniele Landi. "Modeling and thermal simulation of a PHEV battery module with cylindrical LFP cells." *World Electric Vehicle Journal* 6, no. 1 (2013): 175-185. <https://doi.org/10.3390/wevj6010175>
- [4] Pérez, G., I. Gandiaga, M. Garmendia, J. F. Reynaud, and U. Viscarret. "Modelling of Li-ion batteries dynamics using impedance spectroscopy and pulse fitting: EVs application." *World Electric Vehicle Journal* 6, no. 3 (2013): 644-652. <https://doi.org/10.1109/EVS.2013.6914973>
- [5] Berrueta, Alberto, Víctor Irigaray, Pablo Sanchis, and Alfredo Ursúa. "Lithium-ion battery model and experimental validation." In *2015 17th European Conference on Power Electronics and Applications (EPE'15 ECCE-Europe)*, pp. 1-8. IEEE, 2015. <https://doi.org/10.1109/EPE.2015.7309337>
- [6] Hinz, Hartmut. "Comparison of lithium-ion battery models for simulating storage systems in distributed power generation." *Inventions* 4, no. 3 (2019): 41. <https://doi.org/10.3390/inventions4030041>
- [7] Bryden, Thomas S., Borislav Dimitrov, George Hilton, Carlos Ponce de León, Peter Bugryniec, Solomon Brown, Denis Cumming, and Andrew Cruden. "Methodology to determine the heat capacity of lithium-ion cells." *Journal of Power Sources* 395 (2018): 369-378.
- [8] Coman, Paul T., Sean Rayman, and Ralph E. White. "A lumped model of venting during thermal runaway in a cylindrical Lithium Cobalt Oxide lithium-ion cell." *Journal of Power Sources* 307 (2016): 56-62. <https://doi.org/10.1016/j.jpowsour.2015.12.088>
- [9] Lin, Xinfan, Hector E. Perez, Shankar Mohan, Jason B. Siegel, Anna G. Stefanopoulou, Yi Ding, and Matthew P. Castanier. "A lumped-parameter electro-thermal model for cylindrical batteries." *Journal of Power Sources* 257 (2014): 1-11. <https://doi.org/10.1016/j.jpowsour.2014.01.097>
- [10] Panchal, Satyam, Scott Mathewson, Roydon Fraser, Richard Culham, and Michael Fowler. *Measurement of temperature gradient (dT/dy) and temperature response (dT/dt) of a prismatic lithium-ion pouch cell with LiFePO<sub>4</sub> cathode material*. No. 2017-01-1207. SAE Technical Paper, 2017. <https://doi.org/10.4271/2017-01-1207>



- [11] Ahmadou Samba, Ahmadou, Noshin Omar, Hamid Gualous, Peter Van den Bossche, Joeri Van Mierlo, and Tala Ighil Boubekeur. "Development of 2D thermal battery model for Lithium-ion pouch cells." *World Electric Vehicle Journal* 6, no. 3 (2013): 629-637. <https://doi.org/10.3390/wevj6030629>
- [12] Xia, Quan, Zili Wang, Yi Ren, Bo Sun, Dezhen Yang, and Qiang Feng. "A reliability design method for a lithium-ion battery pack considering the thermal disequilibrium in electric vehicles." *Journal of Power Sources* 386 (2018): 10-20. <https://doi.org/10.1016/j.jpowsour.2018.03.036>
- [13] Madani, Seyed Saeed, Maciej Swierczynski, and Søren Knudsen Kær. "Cooling simulation and thermal abuse modeling of lithium-ion batteries using the Newman, Tiedemann, Gu, and Kim (NTGK) model." *ECS Transactions* 81, no. 1 (2017): 261. <https://doi.org/10.1149/08101.0261ecst>
- [14] Li, Genong, Shaoping Li, and Jing Cao. "Application of the MSMD framework in the simulation of battery packs." In *ASME International Mechanical Engineering Congress and Exposition*, vol. 46569, p. V08BT10A026. American Society of Mechanical Engineers, 2014. <https://doi.org/10.1115/IMECE2014-39882>
- [15] Panchal, S., M. Haji Akhondzadeh, K. Raahemifar, M. Fowler, and R. Fraser. "Heat and mass transfer modeling and investigation of multiple LiFePO<sub>4</sub>/graphite batteries in a pack at low C-rates with water-cooling." *International Journal of Heat and Mass Transfer* 135 (2019): 368-377. <https://doi.org/10.1016/j.ijheatmasstransfer.2019.01.076>
- [16] Zhou, Haobing, Fei Zhou, Lipeng Xu, and Jizhou Kong. "Thermal performance of cylindrical Lithium-ion battery thermal management system based on air distribution pipe." *International Journal of Heat and Mass Transfer* 131 (2019): 984-998. <https://doi.org/10.1016/j.ijheatmasstransfer.2018.11.116>
- [17] Zhao, Gang, Xiaolin Wang, Michael Negnevitsky, and Hengyun Zhang. "A review of air-cooling battery thermal management systems for electric and hybrid electric vehicles." *Journal of Power Sources* 501 (2021): 230001. <https://doi.org/10.1016/j.jpowsour.2021.230001>
- [18] Rao, Zhonghao, Zhen Qian, Yong Kuang, and Yimin Li. "Thermal performance of liquid cooling based thermal management system for cylindrical lithium-ion battery module with variable contact surface." *Applied Thermal Engineering* 123 (2017): 1514-1522. <https://doi.org/10.1016/j.applthermaleng.2017.06.059>
- [19] Deng, Yuanwang, Changling Feng, E. Jiaqiang, Hao Zhu, Jingwei Chen, Ming Wen, and Huichun Yin. "Effects of different coolants and cooling strategies on the cooling performance of the power lithium ion battery system: A review." *Applied Thermal Engineering* 142 (2018): 10-29. <https://doi.org/10.1016/j.applthermaleng.2018.06.043>
- [20] Buidin, Thomas Imre Cyrille, and Florin Mariasiu. "Battery thermal management systems: Current status and design approach of cooling technologies." *Energies* 14, no. 16 (2021): 4879. <https://doi.org/10.3390/en14164879>
- [21] Liu, Changcheng, Dengji Xu, Jingwen Weng, Shujia Zhou, Wenjuan Li, Yongqing Wan, Shuaijun Jiang, Dechuang Zhou, Jian Wang, and Que Huang. "Phase change materials application in battery thermal management system: a review." *Materials* 13, no. 20 (2020): 4622. <https://doi.org/10.3390/ma13204622>
- [22] Behi, Hamidreza, Danial Karimi, Mohammadreza Behi, Joris Jaguemont, Morteza Ghanbarpour, Masud Behnia, Maitane Berecibar, and Joeri Van Mierlo. "Thermal management analysis using heat pipe in the high current discharging of lithium-ion battery in electric vehicles." *Journal of energy storage* 32 (2020): 101893. <https://doi.org/10.1016/j.est.2020.101893>
- [23] Ye, Ben, Md Rashedul Haque Rubel, and Hongjun Li. "Design and optimization of cooling plate for battery module of an electric vehicle." *Applied sciences* 9, no. 4 (2019): 754. <https://doi.org/10.3390/app9040754>
- [24] Zhao, Jiateng, Zhonghao Rao, and Yimin Li. "Thermal performance of mini-channel liquid cooled cylinder based battery thermal management for cylindrical lithium-ion power battery." *Energy conversion and management* 103 (2015): 157-165. <https://doi.org/10.1016/j.enconman.2015.06.056>
- [25] Panchal, Satyam, Rocky Khasow, Ibrahim Dincer, Martin Agelin-Chaab, Roydon Fraser, and Michael Fowler. "Thermal design and simulation of mini-channel cold plate for water cooled large sized prismatic lithium-ion battery." *Applied Thermal Engineering* 122 (2017): 80-90. <https://doi.org/10.1016/j.applthermaleng.2017.05.010>
- [26] Huo, Yutao, Zhonghao Rao, Xinjian Liu, and Jiateng Zhao. "Investigation of power battery thermal management by using mini-channel cold plate." *Energy Conversion and Management* 89 (2015): 387-395. <https://doi.org/10.1016/j.enconman.2014.10.015>
- [27] Prajapati, Yogesh K., Manabendra Pathak, and Mohd Kaleem Khan. "A comparative study of flow boiling heat transfer in three different configurations of microchannels." *International Journal of Heat and Mass Transfer* 85 (2015): 711-722. <https://doi.org/10.1016/j.ijheatmasstransfer.2015.02.016>
- [28] Fluent Ansys, "Ansys Fluent Theory Guide," ANSYS Inc., USA, vol. 15317, no. November, pp. 724-746, 2013.
- [29] Paccha-Herrera, Edwin, Williams R. Calderón-Muñoz, Marcos Orchard, Francisco Jaramillo, and Kamal Medjaher. "Thermal Modeling Approaches for a LiCoO<sub>2</sub> Lithium-ion Battery—A Comparative Study with Experimental Validation." *Batteries* 6, no. 3 (2020): 40. <https://doi.org/10.3390/batteries6030040>